European Review for Medical and Pharmacological Sciences 2019; 23: 6645-6656

CX3CR1 participates in pulmonary angiogenesis in experimental hepatopulmonary syndrome mice through inhibiting AKT/ERK signaling pathway and regulating NO/NOS release

H.-J. GU[1], S. ZUO[1], H.-Y. LIU[1], L.-L. GU[1], X.-W. YANG[1], J. LIAO[1], Q.-Q. WANG[1], R. ZHAO[1], X.-S. FENG[2], H.-Y. LI[1]

[1]Department of Hepatobiliary Surgery, Affiliated Hospital of Guizhou Medical University, Yunyan District, Guiyang, P.R. China
[2]Department of Hepatobiliary Surgery, Union Hospital, Tongji Medical College, Huazhong University of Science and Technology, Jiangan District, Wuhan, P.R. China

Huajian Gu, Shi Zuo, and Haiyuan Liu contributed equally to this work

Abstract. – OBJECTIVE: Hepatopulmonary syndrome (HPS) is a kind of pulmonary microvascular disease and occurs in 15%-30% cirrhosis. This study aimed to investigate the effects of pulmonary CX3CR1 on angiogenesis and associated mechanisms in HPS animal models.

MATERIALS AND METHODS: CX3CR1GFP/GFP mice were constructed by replacing CX3CR1 with GFP. Common bile duct ligation (CBDL) mouse model was established with surgery. Release of nitric oxide (NO) was evaluated. Hematoxylin-eosin (HE) staining was employed to examine the inflammation of lung tissues. CD31 expression was detected with immunohistochemistry assay. Western blotting was used to evaluate the expression of CX3CL1, CX3CR1, phosphorylated-AKT (p-AKT), phosphorylated-ERK (p-ERK). Quantitative Real Time-PCR (qRT-PCR) assay was used to examine VEGF, PDGF, iNOS, eNOS, and HO-1 expression.

RESULTS: CX3CR1-deficiency (CX3CR1GFP/GFP-sham or CX3CR1GFP/GFP-CBDL mice) significantly reduced NO release compared to wide type (WT)-mice or WT-CBDL mice ($p<0.05$). CX3CR1-deficiency significantly alleviated inflammation compared to wide type (WT)-mice or WT-CBDL mice ($p<0.05$). CX3CR1-deficiency significantly reduced CD31 expression compared to WT-sham and WT-CBDL mice, respectively ($p<0.05$). CX3CR1 also participated in anti-angiogenesis efficacy of Bevacizumab. CX3CR1-deficiency significantly down-regulated the ratio of p-AKT/AKT and p-ERK/ERK and inhibited the secretion of VEGF and PDGF compared to WT-mice ($p<0.05$). CX3CR1-deficiency significantly reduced iNOS, eNOS, and HO-1 expression compared to WT-mice ($p<0.05$).

CONCLUSIONS: CX3CR1 deficiency reduced VEGF and PDGF production, inhibited p-AKT, and p-ERK activation and down-regulated iNOS, eNOS, and HO-1 expression. Therefore, CX3CR1 participates in pulmonary angiogenesis in the experimental HPS mice via inhibiting AKT/ERK signaling pathway and regulating NO/NOS release. These findings would provide a potential insight for clarifying the pathological mechanisms of HPS.

Key Words:
CX3CR1, Pulmonary angiogenesis, Hepatopulmonary syndrome, Common bile duct ligation.

Introduction

Hepatic dysfunction and liver cirrhosis mainly influence the vascular system in many organ systems and impair the functions of organs, and finally cause the enhanced mortality and morbidity[1,2]. Hepatopulmonary syndrome (HPS) is a kind of pulmonary microvascular disease that occurs when arterial oxygenation is impaired by the changes of pulmonary microvasculature in 15% to 30% cirrhosis patients[3,4]. The occurrence of HPS seriously declines the life quality and no effective drugs or therapeutic

Corresponding Author: Huajian Gu, MD; email: zhaoyaree@sina.com

strategies are candidate until now to improve it[5]. However, the limited acknowledges of the pathogenesis of the changed vascular system in HPS, prevent the development for the effective treatments of HPS.

The commonly established and used HPS animal model reproducing abnormal physiologies of human disorders is the chronic common bile duct ligation (CBDL)[6]. The CBDL models mainly exhibit the characteristics of vascular remodeling and pulmonary microvascular dilations. The vascular remodeling is associated with the expression of vascular endothelial growth factor (VEGF) and intra-vascular monocyte accumulation[7], while the pulmonary microvascular dilations are correlated with the PKB/AKT independent activation of the endothelial nitric oxide synthase/nitric oxide (eNOS/NO)[8]. However, the specific mechanism involving in the pathogenesis of HSP has not been fully clarified.

The chemokine, fractalkine (FKN), has been discovered and identified in the 1990s, and illustrates specific characteristics[9]. The FKN includes a CX3C chemokine domain, which constitutes the CX3C family, including CX3C motif-ligand 1 (CX3CL1) and CX3C motif receptor 1 (CX3CR1)[10]. FKN usually expresses on the dendritic cells, endothelial cells, and neurons, and CX3CR1 mainly expresses on the undefined NK or T cells and monocytes[11]. Meanwhile, the FKN closely interacts with the CX3CR1 with higher affinity, the process of which mediates the plenty of biological activities[12]. Zhang et al[13] also reported that the CX3CL1 and CX3CR1 are enhanced in the pulmonary microvascular system of CBDL animal models and trigger the angiogenesis. Normally, the CX3CR1 could interact with CX3CL1 in vascular endothelial cells to activate the angiogenesis by activating the ERK and AKT signaling pathway[14]. The above backgrounds demonstrate that the CX3CR1 and/or CX3CL1 expression and interaction might be associated with the angiogenesis in the CDBL model of HPS.

This study aimed to investigate the effects of the pulmonary CX3CR1 expression or associated signaling pathways on the angiogenesis in the HPS animal models (CBDL models). In this study, we observed the pulmonary NO levels, CX3CR1 expression, and neovascularization, and evaluated the effects of anti-CX3CR1 antibody (Ab) and/or Bevacizumab treatments on the angiogenesis of the HPS animal model.

Materials and Methods

Generation of CX3CR1GFP/GFP Mice

The Balb/C mice, aging from 6-8 weeks, weighting from 20 to 25 g, were used in this study. The CX3CR1$^{GFP/GFP}$ Balb/C mice were purchased from Jackson Immuno Research Labs (West Grove, PA, USA), which were generated according to the previous study[10]. The genotypes of mice were identified and checked by using the PCR assay. The normal mice and the CX3CR1$^{GFP/GFP}$ mice were feed in the optimal environments supplementing with 40-50% humidity and 12 h dark/light cycle. All the *in vivo* tests or experiments were conducted according to the NIH guidelines for the use of laboratory animals. This study was approved by the Affiliated Hospital of Guizhou Medical University, Guiyang, China.

Establishment of CBDL Mouse Model and Trial Grouping

The Balb/C mice, aging from 6-8 weeks, weighting from 20 to 25 g, were employed to establish the CBDL model. The CBDL mouse model (WT-CBDL group or CX3CR1$^{GFP/GFP}$-CBDL group) was established by using the common bile duct ligation, according to the procedures of CBDL surgery described in the previous study[15]. Meanwhile, the sham mice were established by mobilizing with common bile duct without the ligation (for WT-sham group or CX3CR1$^{GFP/GFP}$ sham group). One week post the CBDL or sham surgery, the WT-mice were intraperitoneally injected by using the Bevacizumab (Cat. No. A2006, Selleck Chemicals, Houston, TX, USA, WT-CBDL+Bevacizumab group or CX3CR1$^{GFP/GFP}$-CBDL-Bevacizumab group) and rabbit anti-CX3CR1 neutralizing polyclonal antibody (Cat. No. ab8021, Abcam Biotechnology, Cambridge, MA, USA, WT-CBDL+Ab group) at final concentration of 80 μg/kg body weight per day for one week. Meanwhile, the WT-mice intraperitoneally injected with both Bevacizumab (80 μg/kg·d) and rabbit anti-CX3CR1 neutralizing polyclonal antibody (80 μg/kg·d) were assigned as WT-CBDL+Ab+Bevacizumab group. One week later, the lung samples of mice were collected and analyzed.

Evaluation of NO Levels

The lung tissues of that above mice were ultrasonically homogenized and centrifuged at a speed

of 2500 r/min at 4°C for 10 min. The NO in the supernatants of lung tissues were immediately evaluated with Griess test by using NO Detection kit (Cat. No. A012, Nanjing Jiancheng Biotechnology, Nanjing, China) according to the instruction of the manufacturer. The equal amounts of the above samples were added, and the reagents were mixed and incubated in the 96-well plates (Corning-Costar, Corning, NY, USA) at 37 for 30 min. The absorbance was detected at the wavelength of 540 nm. The amounts of the nitrate were analyzed and calculated by constructing a standard curve.

Hematoxylin-Eosin (HE) Staining

The isolated lung tissues were isolated and sectioned into slices with a thickness of 0.5 μm. Then, the slices were stained by using hematoxylin (Nanjing Jiancheng Biotechnology, Nanjing, China) and eosin (Beyotime Biotechnology, Shanghai, China) and captured with inverted microscopy (Mode: IX81, Olympus, Tokyo, Japan). Finally, the HE staining images were analyzed with Image Pro software (version: Plus 6.0, Media Cybernetics, Inc., Bethesda, MD, USA).

Immunohistochemistry Assay

The isolated lung tissues were isolated and sectioned into slices with a thickness of 0.5 μm. The slices were fixed using 4% paraformaldehyde (Beyotime Biotechnology, Shanghai, China) for 15 min at 37°C. The slices were washed by using Phosphate-Buffered Saline (PBS) and the endogenous peroxidase was inactivated with 3% hydrogen peroxide (Beyotime Biotechnology, Shanghai, China) at 37°C for 5 min. Then, the slices were blocked by using 5% bovine serum albumin (BSA, Beyotime Biotechnology,) at 37°C for 15 min and incubated by using rabbit anti-mouse CD31 monoclonal antibody (1:3000, Cat. No. #59818, Cell Signaling Technology, Beverly, MA, USA) at 4°C overnight. Then, the slices were washed by using PBS and incubated with Biotin-conjugated goat anti-rabbit IgG (1:1000, Cat. No. ab6721, Abcam Biotechnology, Cambridge, MA, USA) at 37°C for 1 h. Finally, the slices were captured by using an inverted fluorescence microscope (Mode: IX81, Olympus, Tokyo, Japan).

Western Blot Assay

The lung tissues were lysed by using radioimmunoprecipitation assay solution (RIPA, Beyotime Biotechnology, Shanghai, China) due to the instruction of the manufacturer. The lysates were separated by using 15% SDS-PAGE (Amresco Inc., Solon, OH, USA) and electro-transferred onto polyvinylidene difluoride (PVDF; Amresco Inc., Solon, OH, USA). The PVDF membranes were blocked by utilizing the 5% defatted milk (Beyotime Biotechnology, Shanghai, China) in PBS containing 0.05% Tween-20 (Beyotime Biotechnology, Shanghai, China). Then, the PVDF membranes were incubated by using rabbit anti-mouse CX3CL1 polyclonal antibody (1:2000, Cat. No. ab25091), rabbit anti-mouse AKT polyclonal antibody (1:2000, Cat. No. ab8805), rabbit anti-mouse phosphorylated AKT (p-AKT) polyclonal antibody (1:2000, Cat. No. ab38449), rabbit anti-mouse ERK polyclonal antibody (1:2000, Cat. No. ab17942), rabbit anti-mouse phosphorylated ERK (p-ERK) polyclonal antibody (1:2000, Cat. No. ab201015), rabbit anti-mouse CX3CR1 polyclonal antibody (1:2000, Cat. No. 13885-1-AP, Wuhan Sanying, Wuhan, China), and rabbit anti-mouse β-actin polyclonal antibody (1: 2000, Cat. No. ab8227) at 4°C overnight. All the primary antibodies except for rabbit anti-mouse CX3CR1 were purchased from Abcam Biotechnology (Cambridge, MA, USA). The PVDF membranes were then incubated with the horseradish peroxidase (HRP)-conjugated goat anti-rabbit IgG antibody (1:2000, Cat. No. AP132, Sigma-Aldrich, St. Louis, MO, USA). The bands of the Western blotting were visualized and captured with a BeyoECL Plus kit (Cat. No. P0018M, Beyotime Biotechnology, Shanghai, China). Finally, the binds or signals of the Western blotting images were analyzed by using the UVP Western-blotting gel-scanning system (Mode: GDS8000, UVP, Sacramento, CA, USA).

Quantitative Real-Time RT-PCR (qRT-PCR) Assay

The total RNAs in lung tissues were extracted with the TRIzol reagents (Beyotime Biotechnology, Shanghai, China), and then it was used as the templates to synthesize complementary DNAs (cDNAs) with the Reverse-Transcription kit (Western Biotechnology, Chongqing, China) based on the manufacturer's instruction. The qRT-PCR assay was conducted with the Sybgreen I kit (Western Biotechnology, Chongqing, China) as fluorescent-dye, on a Real Time-PCR device (Mode: FTC-3000P, Funglyn Biotechnology, Richmond Hill, Ontario, Canada). The primers for the qRT-PCR assay, including VEGF, PDGF, iNOS, eNOS, HO-1, and β-actin were listed in Table I. PCR products of the amplification were loaded onto the 2% agarose gels (Beyotime Bio-

technology, Shanghai, China). The gel images of PCR amplification were analyzed with UVP Western-blotting gel-scanning system (Mode: GDS8000, UVP, Sacramento, CA, USA). The relative gene mRNA levels were calculated by normalizing to the inter-control β-actin gene with the comparative threshold cycle $2^{-\Delta\Delta CT}$ method[16].

Statistical Analysis

The data appeared in this study was represented as mean ± standard deviation (SD) and analyzed using SPSS software 20.0 (IBM Corp., Armonk, NY, USA). The Tukey's post-hoc test validated the analysis of variance (ANOVA) and was used to compare the data among multiple groups. The $p<0.05$ represented a significant difference.

Results

CX3CR1-deficiency (CX3CR1$^{GFP/GFP}$ mice) reduced NO release

NO has been considered to be the pathological factor for many diseases, such as influenza[17], cerebral disorders[18], and cardiovascular diseases[19]. Therefore, the NO levels were evaluated in the tissues of mice. The results indicated that the levels of NO in WT-CBDL mice were significantly increased compared to that in the WT-sham mice (Figure 1, $p<0.05$). However, the Ab combining Bevacizumab treatment (WT-CBDL+Ab+Bevacizumab group) significantly enhanced the NO levels compared to that in the WT-CBDL group (Figure 1, $p<0.05$). Meanwhile, the CX3CR1-deficiency (CX3CR1$^{GFP/GFP}$ mice) also reduced the NO levels compared to that in the WT-sham group (Figure 1, $p<0.05$). The NO levels in CX3CR1-deficiency CBDL mice (CX3CR1$^{GFP/GFP}$-CBDL mice) were significantly lower compared to that in WT-CBDL mice (Figure 1, $p<0.05$). Also, the Bevacizumab treatment (CX3CR1$^{GFP/GFP}$-CBDL+ Bevacizumab group) significantly decreased the NO levels compared to CX3CR1$^{GFP/GFP}$-CBDL group (Figure 1, $p<0.05$).

CX3CR1-Deficiency (CX3CR1GFP/GFP Mice) Decreased the Inflammation

The results showed that CBDL mice model exhibited evident inflammation in lung tissues compared to the WT-sham mice (Figures 2A and 2B, $p<0.05$), which also confirmed the successful establishment of CBDL mice model. The Ab and Bevacizumab treatment significantly decreased the inflammation in lung tissues compared to that in the WT-CBDL group (Figures 2A and 2B, $p<0.05$). Meanwhile, CX3CR1-deficiency (CX3CR1$^{GFP/GFP}$-sham mice or CX3CR1$^{GFP/GFP}$-CBDL mice) significantly decreased the inflammation compared to that in the WT-sham and WT-CBDL mice (Figures 2A and 2B, $p<0.05$). Furthermore, the Bevacizumab strengthened the effects of CX3CR1-deficiency on inflammation (Figures 2A and 2B).

CX3CR1-Deficiency (CX3CR1$^{GFP/GFP}$ Mice) Reduced CD31 Expression

CD31 is a specific biomarker for the vascular endothelial cells, the enhanced CD31 levels reflect the vascular injury in a feedback way [20]. Our results indicated that CX3CR1-deficiency inhibited the up-regulated effects of CBDL injury on the WT-sham mice, by suppressing the

Table I. Primers for the RT-PCR assay.

Genes		Sequences	Length (bp)
VEGF	Forward	ATCATGCGGATCAAACCTCAC	96
	Reverse	TGTTCTGTCTTTCTTTGGTCTGC	
PDGF	Forward	CGCACCAACGCCAACTTC	154
	Reverse	TGGGCTTCTTTCGCACAATC	
iNOS	Forward	TTGGAGCGAGTTGTGGATTG	147
	Reverse	GGTCGTAATGTCCAGGAAGTAGG	
eNOS	Forward	ACAAATAGAGGCAATCTTCGTTC	110
	Reverse	CTATAGCCCGCATAGCGTATC	
HO-1	Forward	CGAATGAACACTCTGGAGATGAC	166
	Reverse	GCCTCTGACGAAGTGACGC	
β-actin	Forward	GAGACCTTCAACACCCCAGC	263
	Reverse	ATGTCACGCACGATTTCCC	

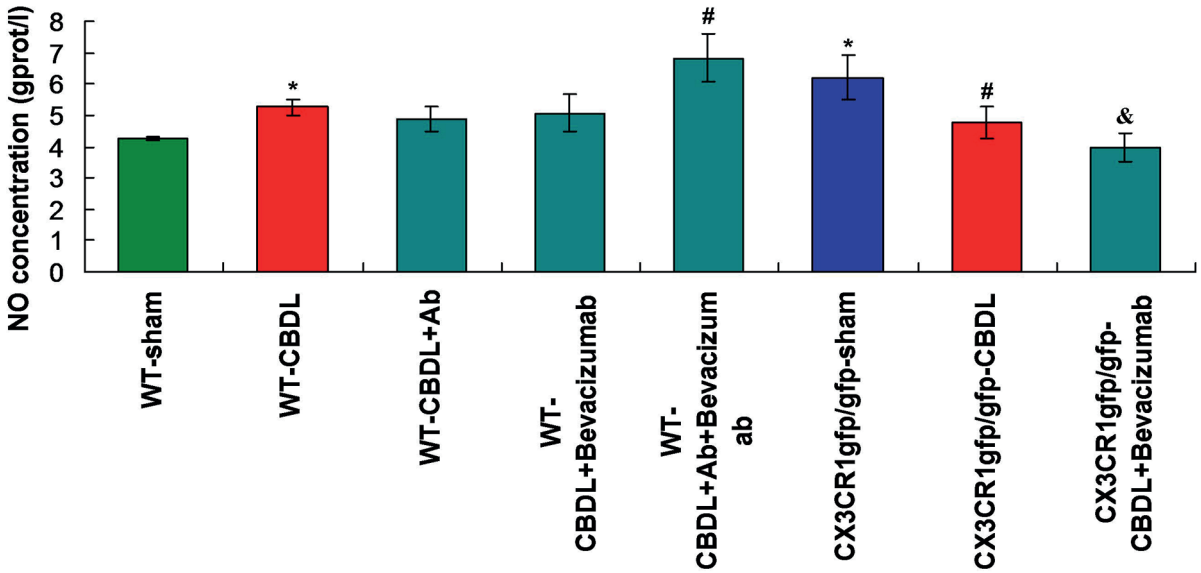

Figure 1. Evaluation for the NO release in the WT mice and the CX3CR1-deficiency (CX3CR1$^{GFP/GFP}$ mice) mice. $^{*}p<0.05$ *vs.* WT-sham group. $^{\#}p<0.05$ *vs.* WT-CBDL group. $^{\&}p<0.05$ *vs.* CX3CR1$^{GFP/GFP}$-CBDL group.

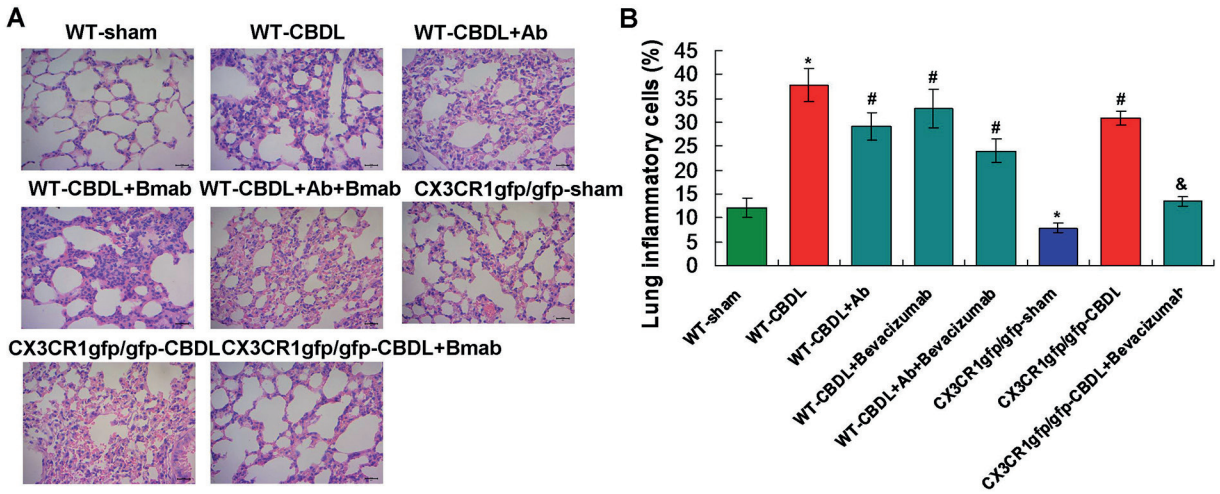

Figure 2. Determination of the inflammation of the lung tissues of WT mice and the CX3CR1-deficiency (CX3CR1$^{GFP/GFP}$ mice) mice by using HE staining. ***A,*** HE staining images (magnification x400). ***B,*** Statistical analysis for the inflammation. $^{*}p<0.05$ *vs.* WT-sham group. $^{\#}p<0.05$ *vs.* WT-CBDL group. $^{\&}p<0.05$ *vs.* CX3CR1$^{GFP/GFP}$-CBDL group.

CD31 expression (Figure 3A). Meanwhile, the CD31 levels in CX3CR1$^{GFP/GFP}$-CBDL mice were significantly reduced compared to that in the WT-CBDL group (Figure 3B, $p<0.05$). Moreover, the Bevacizumab assisted the effects of CX3CR1 on the downregulation of CD31 (Figure 3B).

CX3CR1 Participated in the Efficacy of Bevacizumab

In the CX3CR1-deficiency (CX3CR1$^{GFP/GFP}$ mice) mice, the CX3CL1 was down-regulated compared to that in the WT-sham and WT-CBDL mice (Figures 4A and 4B, $p<0.05$). The results also indicated that the CX3CL1 expres-

sion in both WT-CBDL+Bevacizumab group and CX3CR1$^{GFP/GFP}$-CBDL+Bevacizumab were significantly decreased compared to that in the WT-sham mice and WT-CBDL mice, respectively (Figures 4A and 4B, $p<0.05$). Meanwhile, there were no expressions of CX3CR1 in the CX3CR1$^{GFP/GFP}$-sham, CX3CR1$^{GFP/GFP}$-CBDL, and CX3CR1$^{GFP/GFP}$-CBDL-Bevacizumab group (Figures 4A and 4C, $p<0.05$). These results suggest that the Bevacizumab played protective effects against the CBDL by downregulating the CX3CR1 expression.

CX3CR1-Deficiency (CX3CR1$^{GFP/GFP}$ Mice) Down-Regulated Ratio of p-AKT/AKT and p-ERK/ERK

Due to the roles of AKT and ERK in the CX3CR1 associated angiogenesis[14], the p-AKT/AKT and p-ERK/ERK ratios were calculated. We found that both of p-AKT/AKT and p-ERK/ERK ratios were down-regulated in CX3CR1$^{GFP/GFP}$-sham and CX3CR1$^{GFP/GFP}$-CBDL mice compared to that in the WT-sham mice and CX3CR1-CBDL mice, respectively (Figures 5A, 5B, 5C, $p<0.05$). These results suggest that the CX3CR1-deficiency inhibited the AKT/ERK signaling pathway in the CX3CR1 associated angiogenesis.

CX3CR1-Deficiency (CX3CR1$^{GFP/GFP}$ Mice) Inhibited Secretion of VEGF and PDGF

In our study, the angiogenesis-related molecules, VEGF and PDGF, were examined by using qRT-PCR assay. The results indicated that the establishment of CBDL models triggered the secretion of VEGF and PDGF (Figures 6A and 6B). However, the CX3CR1-deficiency (both CX3CR1$^{GFP/GFP}$-sham mice and CX3CR1$^{GFP/GFP}$-CBDL mice) significantly reduced the VEGF and

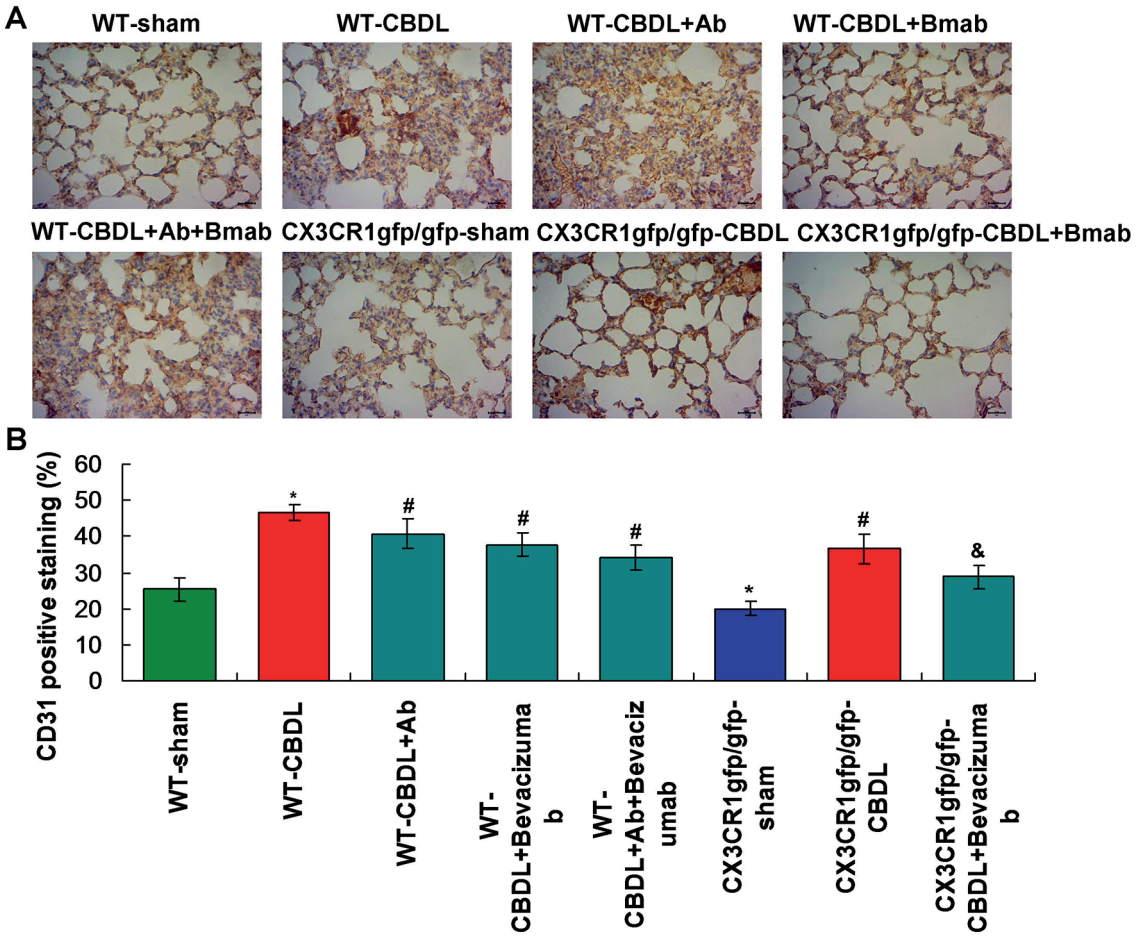

Figure 3. CX3CR1-deficiency reduced the CD31 expression according to the immunohistochemistry assay. ***A***, Immunohistochemistry assay images (magnification x400). ***B***, Statistical analysis for the CD expression. $^{*}p<0.05$ *vs.* WT-sham group. $^{\#}p<0.05$ *vs.* WT-CBDL group. $^{\&}p<0.05$ *vs.* CX3CR1$^{GFP/GFP}$-CBDL group.

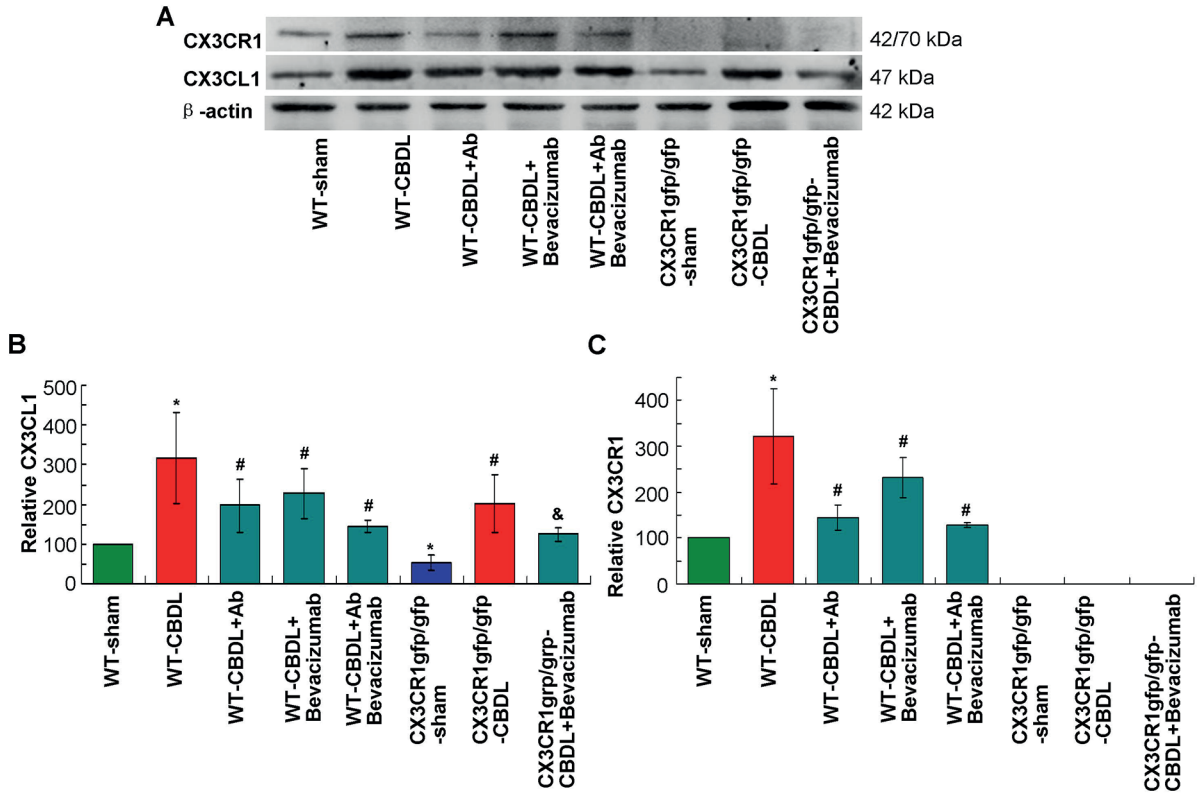

Figure 4. Evaluation for CX3CR1 and CX3CL1 expression using Western blotting assay. ***A,*** Western blotting images. ***B,*** Statistical analysis for the CX3CL1 expression. ***C,*** Statistical analysis for the CX3CR1 expression. $^{*}p<0.05$ *vs.* WT-sham group. $^{\#}p<0.05$ *vs.* WT-CBDL group. $^{\&}p<0.05$ *vs.* CX3CR1$^{GFP/GFP}$-CBDL group.

PDGF secretion compared to that in the WT-sham mice and WT-CBDL mice, respectively (Figures 6A and 6B, $p<0.05$). Meanwhile, the Bevacizumab blocked the effects of CX3CR1-deficiency on VEGF and PDGF secretion (Figures 6A and 6B).

CX3CR1-Deficiency (CX3CR1$^{GFP/GFP}$ Mice) Reduced iNOS, eNOS, and HO-1 Expression

The expressions of iNOS, eNOS, and HO-1 were also detected in the lung tissues by using the qRT-PCR assay. The results illustrated that iNOS (Figure 7A), eNOS (Figure 7B), and HO-1 (Figure 7C) expressions were significantly increased in WT-CBDL mice compared to that in the WT-sham mice ($p<0.05$). In addition, the CX3CR1-deficiency (both CX3CR1$^{GFP/GFP}$-sham mice and CX3CR1$^{GFP/GFP}$-CBDL mice) significantly decreased the iNOS (Figure 7A), eNOS (Figure 7B), and HO-1 (Figure 7C) expressions compared to that in the WT-sham mice and WT-CBDL-sham mice, respectively ($p<0.05$).

Discussion

In the progression of HPS, the hepatic cirrhosis or portal hypertension might cause pulmonary vascular remodeling[21]. The previous studies[22,23] reported that many cytokines and signaling pathways participate in the pathogenesis of HPS. However, there are only a few investigations exploring the signaling pathways that relate to the HPS which caused pulmonary vascular remodeling till now. According to the former reports[24-26], the angiogenic processes could be modulated by many negative or positive effectors, such as the chemokines, growth factors, cytokines, or the adhesion molecules. Therefore, in this work, we evaluated the effects of the CX3CR1 on the angiogenesis activation in the HPS animal model. We found that the CX3CR1 expression was increased in the lung tissues of the HPS animal models. The CX3CR1 deficiency in the HPS animal models significantly improved the angiogenesis. There-

fore, the present study provided the insight that the deficient CX3CR1 could reflect the improvement of the experimental HPS and CX3CR1 was identified as a regulator for the HPS.

The common bile duct ligation approach (CBDL model) is a unique animal model for HPS until now, which has been proven to be effective, due to previous studies[13,23,27,28]. Therefore, we employed the CBDL mouse model to clarify the effects of CX3CR1 on angiogenesis by inhibiting the CX3CR1 expression in this study. Moreover, the effects of CX3CR1 blockade (the neutralizing antibody, Ab, and Bevacizumab) on pulmonary abnormalities were also evaluated in the CBDL mouse models. CX3CR1 is encoded by one single exon, which was replaced by the GFP cassette in our established CX3CR1$^{GFP/GFP}$ mice; therefore, the transcripts carrying the un-translated CX3CR1 gene exon splicing onto GFP were generated. By using the above approach, we knocked out or silenced CX3CR1 gene transcription and expression in the CX3CR1$^{GFP/GFP}$ mice, which was also called as CX3CR1-deficiency mice.

In this study, pulmonary inflammation and pulmonary angiogenesis were firstly observed. The results showed that CX3CR1-deficiency (CX3CR1$^{GFP/GFP}$ mice) remarkably decreased the inflammation compared to the wild type mice. Meanwhile, the pulmonary angiogenesis was also evaluated by detecting the CD31 expression. These findings showed that the CD31 expression was significantly inhibited in the CX3CR1-deficiency (CX3CR1$^{GFP/GFP}$ mice) mice compared with the wild type mice or wild type CBDL mice, which were consistent with the previous documents[29,30]. Of note, we also found that the neutralizing antibody and Bevacizumab exhibited equal effects comparing to the CX3CR1-deficiency,

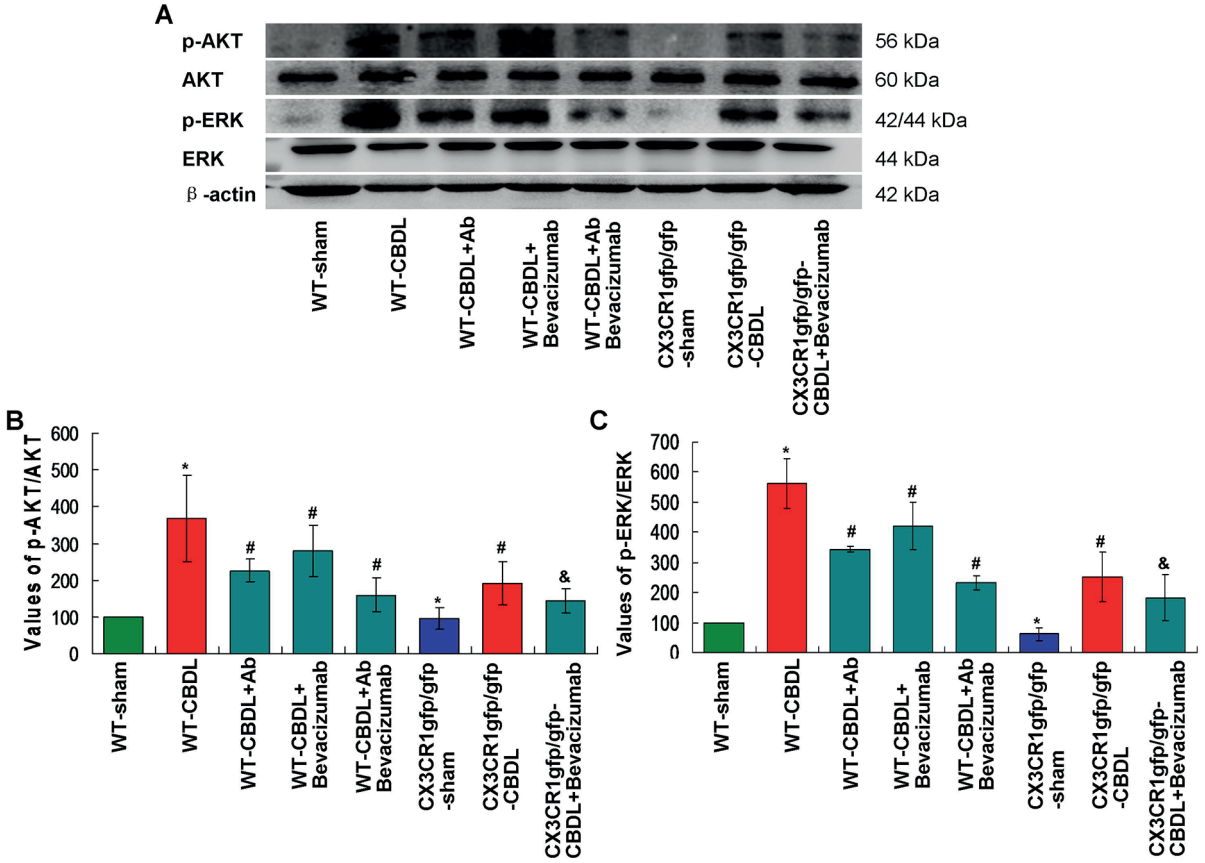

Figure 5. CX3CR1-deficiency inhibited the AKT/ERK signaling pathway in the CBDL mice. ***A,*** Expression of AKT/ERL signaling molecules was examined with Western blotting assay. ***B,*** Statistical analysis for the ratio of p-AKT/AKT. ***C,*** Statistical analysis for the ratio of p-ERK/ERK. $^{*}p<0.05$ *vs.* WT-sham group. $^{\#}p<0.05$ *vs.* WT-CBDL group. $^{\&}p<0.05$ *vs.* CX3CR1$^{GFP/GFP}$-CBDL group.

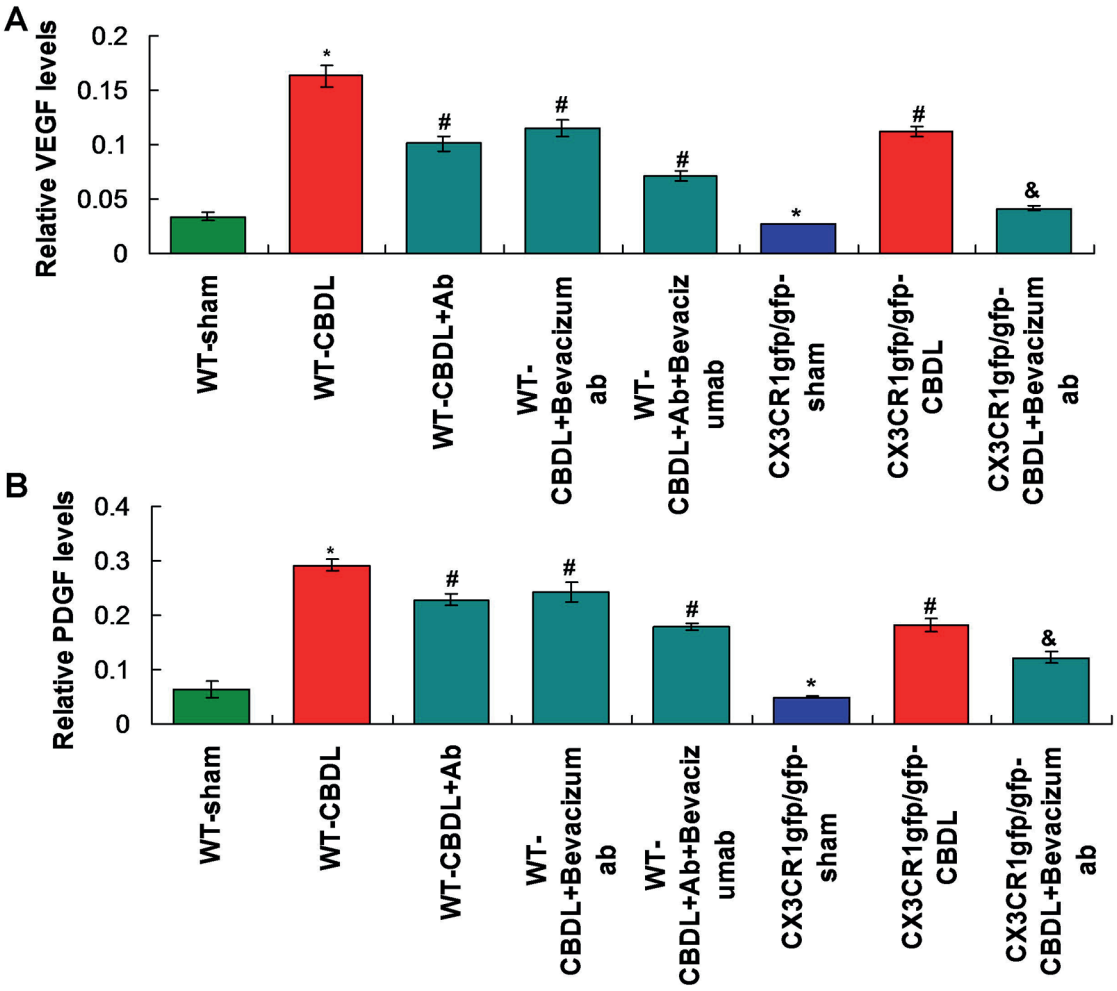

Figure 6. Growth factors detection by using qRT-PCR assay. ***A,*** Statistical analysis for VEGF mRNA expression. ***B,*** Statistical analysis for PDGF mRNA expression. $^{*}p<0.05$ *vs.* WT-sham group. $^{\#}p<0.05$ *vs.* WT-CBDL group. $^{\&}p<0.05$ *vs.* CX3CR1$^{GFP/GFP}$-CBDL group.

which suggest that CXC3R1 could directly affect the CBDL.

Scholars[31,32] reported that the pulmonary vasodilation was associated with the NO/NOS signaling pathway activation in the HPS animal model. Thus, the NO levels and the NO associated iNOS, eNOS, and HO-1 levels were analyzed here. Our results illustrated that all the NO, iNOS, eNOS, and HO-1 levels were significantly decreased in the CX3CR1$^{GFP/GFP}$ mice compared to that in the wide type mice (WT mice). These findings suggest that the CX3CR1 deficiency (CX3CR1$^{GFP/GFP}$ mice) participated in the pulmonary angiogenesis in the experimental HPS mice (CBDL model) by activating the NOS/NO signaling pathways, which are consistent with the conclusions of the former studies[33,34].

Furthermore, we also investigated the growth factors mediated mechanism, through which the CX3CR1 benefits to the angiogenesis in both CX3CR1$^{GFP/GFP}$-sham mice or CX3CR1$^{GFP/GFP}$-CBDL mice. We indicated that the CX3CR1$^{GFP/GFP}$ deficiency inhibited the angiogenesis by reducing the VEGF and PDGF expression, which is consistent with Zhang et al[13]. Meanwhile, there are also two signaling cascades that could regulate the vascular endothelial cell proliferation and migration, including MEK/ERK/Raf signaling pathway and AKT/3-kinase signaling pathway[35,36]. The results showed that CBDL activated p-AKT and p-ERK as the angiogenesis developments were down-regulated by the deficiency of the CX3CR1 gene as the improvement of HPS. The above data suggest that CX3CR1 triggers the activation of the angio-

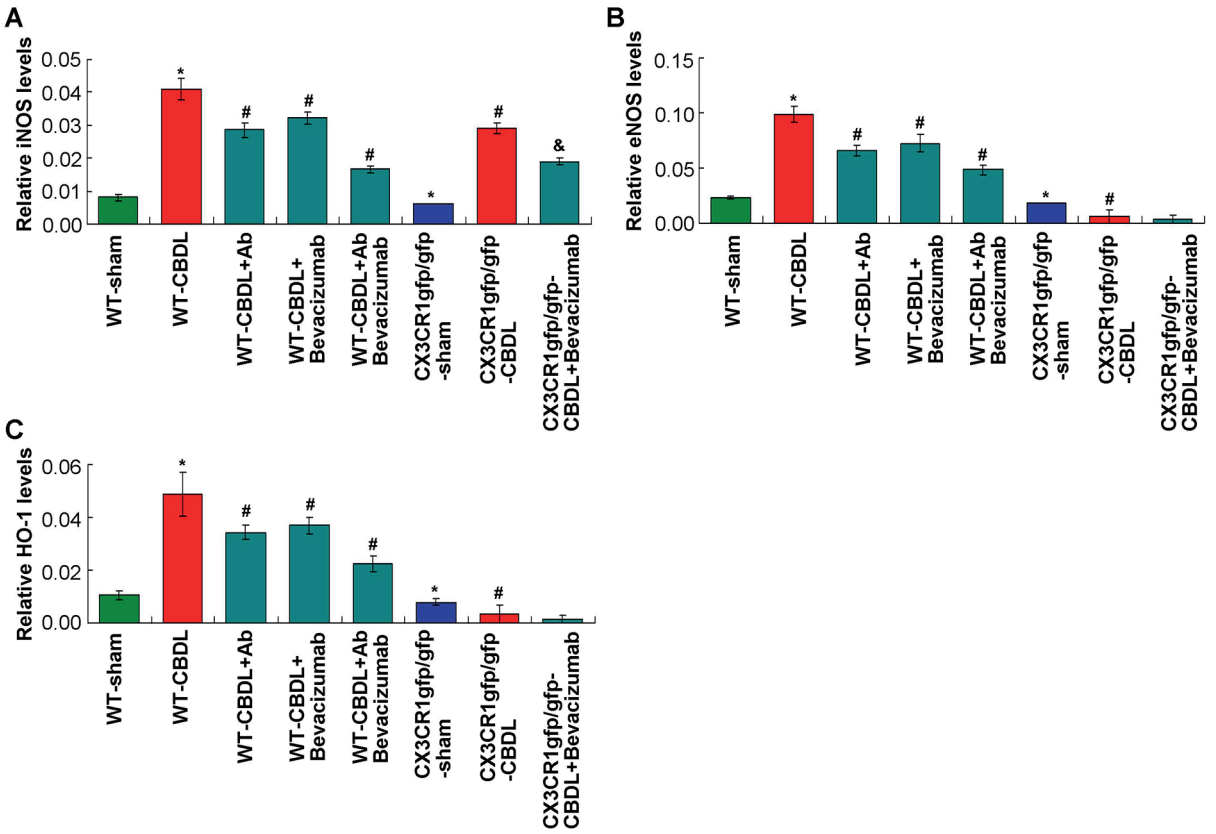

Figure 7. CX3CR1-deficiency reduced the iNOS, eNOS, and HO-1 mRNA expression according to the qRT-PCR assay. ***A,*** Statistical analysis for iNOS mRNA expression. ***B,*** Statistical analysis for eNOS mRNA expression. ***C,*** Statistical analysis for HO-1 expression. $^{*}p<0.05$ *vs.* WT-sham group. $^{\#}p<0.05$ *vs.* WT-CBDL group. $^{\&}p<0.05$ *vs.* CX3CR1$^{GFP/GFP}$-CBDL group.

genic signaling pathways in pulmonary vascular endothelial cells, which contribute to the pathogenesis of the HPS.

Conclusions

We demonstrated that the CX3CR1 levels were significantly increased in the lung tissues during the pulmonary angiogenesis and progression of HPS in the CBDL mouse models. The CX3CR1 deficiency reduced the production of VEGF and PDGF and inhibited the activation of the p-AKT and p-ERK in the vascular endothelial cells of lung tissues. Meanwhile, the CX3CR1 deficiency also down-regulated the iNOS, eNOS, and HO-1 expression in lung tissues of CBDL mice. The present results would provide a potential insight to clarify the pathological mechanisms and to discover the therapeutic strategy for the HPS in the future.

Acknowledgements

This study was granted by the National Natural Science Foundation of China (Grant No. 81560106) and the Basic Research Plan of Guizhou Science and Technology Program (Grant No. [2017]1145).

Conflict of interest

The authors declare no conflicts of interest.

References

1) Zhang J, Fallon MB. Hepatopulmonary syndrome: update on pathogenesis and clinical features. Nat Rev Gastroenterol Hepatol 2012; 9: 539-559.
2) Zhao WX, Liu XM, Yu CM, Xu H, Dai JR, Chen HY, Li L, Chen F, Ou YL, Zhao ZK. Peritoneal dialysis effectively removes toxic substances and improves liver functions of liver failure patients. Eur Rev Med Pharmacol Sci 2018; 22: 2432-2438.

3) Rodriguez-Roisin R, Krowka MJ. Hepatopulmonary syndrome-a liver induced lung vascular disorder. N Engl J Med 2008; 358: 2378-2387.

4) Feng G, Rong H. The role of hemodynamic and vasoactive substances on hepatopulmonary syndrome. Eur Rev Med Pharmacol Sci 2014; 18: 380-386.

5) Fallon MB, Krowka MJ, Brown RS, Trotter JE, Zacks S, Roberts KE, Shah VH, Kaplowitz N, Forman L, Wille K, Kawut SM, Pulmonary Vascular Complications of Liver Disease Study Group. Impact of hepatopulmonary syndrome on quality of life and survival in liver transplant candidates. Gastroenterology 2008; 135: 1168-1175.

6) Thenappan T, Goel A, Marsboom G, Fang YH, Toth PT, Zhang HJ, Kajomoto H, Hong Z, Paul J, Wietholt C, Pogoriler J, Piao L, Rehman J, Archer SL. A central role for CD68(+) macrophages in hepatopulmonary syndrome: reversal by macrophage depletion. Am J Respir Crit Care Med 2011; 183: 1080-1091.

7) Luo B, Tang L, Wang Z, Zhang J, Ling Y, Feng W, Sun JZ, Stockard CR, Frost AR, Chen YF, Grizzle WE, Fallon MB. Cholangiocyte endothelin 1 and transforming growth factor beta 1 production in rat experimental hepatopulmonary syndrome. Gastroenterology 2005; 129: 682-695.

8) Tang L, Luo B, Patel RP, Ling Y, Zhang J, Fallon MB. Modulation of pulmonary endothelial endothelin B receptor expression and signaling: implications for experimental hepatopulmonary syndrome. Am J Physiol Lung Cell Mol Physiol 2007; 292: L1467-L1472.

9) Bazan JF, Bacon KB, Hardiman G, Wang W, Soo K, Rossi D, Greaves DR, Ziotnik A, Schall TJ. A new class of membrane-bound chemokine with a CX3C motif. Nature 1997; 385: 640-644.

10) Jung S, Aliberti J, Graemmel P, Sunshine MJ, Kreutzberg GW, Sher A, Littman DR. Analysis of fractalkine receptor (CX3CR1) function by targeted deletion and green fluorescent protein reporter gene insertion. Mol Cell Biol 2000; 20: 4106-4114.

11) Imai T, Yasuda N. Therapeutic intervention of inflammatory/immune diseases by inhibiting of the fractlkine (CX3CL1)-CX3CR1 pathway. Inflamm Regen 2016; 36: 9.

12) Fong AM, Robinson LA, Steeber DA, Tedder TF, Yoshie O, Imai T, Patel DD. Fractalkine and CX3CR1 mediate a novel mechanism of leukocyte capture, firm adhesion, and activation under physiologic flow. J Exp Med 1998; 188: 1413-1419.

13) Zhang J, Yang W, Luo B, Hu B, Maheshwari A, Fallon MB. The role of CX3CL1/CX3CR1 in pulmonary angiogenesis and intravascular monocyte accumulation in rat experimental hepatopulmonary syndrome. J Hepatol 2012; 57: 752-758.

14) Lee SJ, Namkoong S, Kim YM, Kim CK, Lee H, Ha KS, Chung HT, Kwon YG, Kim YM. Fractalkine stimulates angiogenesis by activating the Raf-1/MEK/ERK- and PI3K/Akt/eNOS-dependent signal pathways. Am J Physiol Heart Circ Physiol 2006; 291: H2836-H2846.

15) Fallon MB, Abrams GA, McGrath JW, Hou Z, Luo B. Common bile duct ligation in the rat: a model of intrapulmonary vasodilatation and hepato-pulmonary syndrome. Am J Physiol 1997; 272 (4 Pt 1): G779-G784.

16) Livak KJ, Schmittgen TD. Analysis of relative gene expression data using real-time quantitative PCR and the 2 (-Delta Delta C(T)) method. Methods 2001; 25: 402-408.

17) Watanabe C, Kawashima H, Takekuma K, Hoshika A, Watanabe Y. Increased nitric oxide production and GFAP expression in the brains of influenza A/NWS virus infected mice. Neurochem Res 2008; 33: 1017-1023.

18) Bal N, Roshchin M, Salozhin S, Balaban P. Nitric oxide upregulates proteasomal protein degradation in neurons. Cell Mol Neurobiol 2017; 37: 763-769.

19) Stephan BCM, harrison SL, Keage HAD, Babateen A, Robinson L, Siervo M. Cardiovascular disease, the nitric oxide pathway and risk of cognitive impairment and dementia. Curr Cardiol Rep 2017; 19: 87.

20) Lertkiatmongkol P, Liao D, Mei H, Hu Y, Newman PJ. Endothelial functions of platelet/endothelial cell adhesion molecule-1 (CD31). Curr Opin Hematol 2016; 23: 253-259.

21) Zhang H, Lv M, Zhao Z, Jia J, Zhang L, Xiao P, Wang L, Li C, Ji J, Tian X, Li X, Fan Y, Lai L, Liu Y, Li B, Zhang C, Liu M, Guo J, Han D, Ji C. Glucose-regulated protein 78 may play a crucial role in promoting the pulmonary microvascular remodeling in a rat model of hepatopulmonary syndrome. Gene 2014; 545: 156-162.

22) Yi B, Zeng J, Wang G, Qian G, Lu K. Annexin A1 protein regulates the expression of PMVEC cytoskeletal proteins in CBDL rat serum-induced pulmonary microvascular remodeling. J Transl Med 2013; 11: 98.

23) Liu C, Chen L, Zeng J, Cui J, Ning JN, Wang GS, Belguise K, Wang X, Qian GS, Lu KZ, Yi B. Bone morphogenic protein-2 regulates the myogenic differentiaiton of PMVECs in CBDL rat serum-induced pulmonary microvacular remodeling. Exp Cell Res 2015; 336: 109-118.

24) Kuźnar-Kamińska B, Mikuła-Pietrasik J, Mały E, Makowska N, Malec M, Tykarski A, Batura-Gabryel H, KsiĐĐek K. Serum form patients with chronic obstructive pulmonary disease promotes proangiogenic behavior of the vascular endothelium. Eur Rev Med Pharmacol Sci 2018; 22: 7470-7481.

25) Aalinkeel R, Nair MP, Sufrin G, Mahajan SD, Chadha KC, Chawda RP, Schwartz SA. Gene expression of antiogenic factors correlates with metastatic potential of prostate cancer cells. Cancer Res 2004; 64: 5311-5321.

26) Quinn KE, Prosser SZ, Kane KK, Ashley RL. Inhibition of chemokine (C-X-C motif) receptor four (CXCR4) at the fetal-maternal interface during early gestation in sheep: alterations in expression of chemokines, angiogenic factors and their receptors. J Anim Sci 2017; 95: 1144-1153.

27) Georgiev P, Jochum W, Heinrich S, Jang JH, Nocito A, Dahm F, Clavien PA. Characterization of time-related changes after experimental bile duct ligation. Br J Surg 2008; 95: 646-656.

28) Zhang J, Yang W, Hu B, Wu W, Fallon MB. Endothelin-1 activation of the endothelial B receptor modulates pulmonary endothelial CX3CL1 and contributes to pulmonary angiogenesis in experimental hepatopulmonary syndrome. Am J Pathol 2014; 184: 1706-18714.

29) Lu P, Li L, Kuno K, Wu Y, Baba T, Li YY, Zhang XX, Mukaida N. Protective roles of the fractakline/CX3CL1-CX3CR1 interactions in alkali-induced corneal neovascularization through enhanced antiangiogenic factor expression. J Immunol 2008; 180: 4283-4291.

30) Kaur S, Sehgal R, Shastry SM, McCaughan G, McGuire HM, Fzaekas St de Groth B, Sarin S, Trehanpati N, Seth D. Circulating endothelial progenitor cells present an inflammatory phenotype and function in patients with alcoholic liver cirrhosis. Front Physiol 2018; 8: 556.

31) Tang L, Luo B, Patel RP, Ling Y, Zhang J, Fallon MB. Modulation of pulmonary endothelial endothelin B receptor expression and signaling: implications for experimental hepatopulmonary syndrome. Am J Physiol Lung Cell Mol Physiol 2007; 292: L1467-L1472.

32) Ling Y, Zhang J, Luo B, Song D, Liu L, Tang L, Stockard C, Grizzle W, Ku D, Fallon MB. The role of endothelin-1 and the endothelin B receptor in the pathogenesis of experimental hepatopulmonary syndrome in the rat. Hepatology 2004; 39: 1593-1602.

33) Liu L, Luo B, Wang Z, Abrams GA, Fallon MB. Endothelin-1 stimulates eNOS expression and activity in rat pulmonary microvascular endothelial cells. Hepatology 2001; 34: 184A.

34) Basso L, Lapointe TK, Iftinca M, Marsters C, Hollenberg MD, Kurrasch DM, Altier C. Granulocyte-colony-stimulating factor (G-CSF) signaling in spinal microglia drives visceral sensitization following colitis. Proc Natl Acad Sci USA 2017; 114: 11235-11240.

35) Bullard LE, Qi X, Penn JS. Role for extracellular signal-responsive kinase-1 and -2 in retinal angiogenesis. Invest Ophthalmol Vis Sci 2003; 44: 1722-1731.

36) Ma J, Ren L, Guo CJ, Wan NJ, Niu DS. Chemerin affects the metabolic and proliferative capabilities of chondrocytes by increasing the phosphorylation of AKT/ERK. Eur Rev Med Pharmacol Sci 2018; 22: 3656-3662.